

On the Origin of Ultraviolet Contrasts on Venus¹

L. D. TRAVIS

Goddard Institute for Space Studies, NASA, New York, N. Y. 10025

(Manuscript received 13 December 1974, in revised form 27 March 1975)

ABSTRACT

Models for the origin of the contrasts in the ultraviolet images of Venus are examined in an attempt to determine the physical differences between light and dark regions fundamental to a clear understanding of the apparent cloud motions. To evaluate the meaning of the wavelength dependence of the contrasts, an improved determination of the spherical albedo curve for Venus in the $0.225 \leq \lambda \leq 1.06 \mu\text{m}$ range is made by fitting appropriate theoretical models to the observations of monochromatic magnitudes as a function of phase angle. It is shown that, because of differences between the spectral dependences of spherical albedo and contrasts, at least one major absorber other than the one causing the contrasts is almost certainly required.

A popular model employing differential Rayleigh scattering due to variations in cloud height can be ruled out, but several classes of models are compatible with present observational evidence. The contrasts and the absorption associated with them may in fact be occurring below, within or above the main visible cloud layer, and thus an unambiguous interpretation of the apparent cloud motions is not possible.

Ground-based observations of the polarization for the regions of contrast may permit the field of acceptable models to be narrowed. Observations planned for the Pioneer Venus orbiter and entry probes should provide the information on local cloud properties and vertical structure necessary to reveal the physical nature of the UV markings.

1. Introduction

Since their discovery by Wright (1927) and Ross (1928) the markings observed on Venus in the ultraviolet have been a feature of considerable interest, primarily because of inferences based upon their behavior. Ground-based observations indicate that the dark regions exhibit a retrograde rotation with a period on the order of 4 days (Boyer and Camichel, 1961; Smith, 1967; Boyer and Guerin, 1969; Scott and Reese, 1972), and the assumption that this represents a real motion of the upper cloud layers is of course implicit. The high-resolution images recently obtained from Mariner 10 (Murray *et al.*, 1974) show a degree of detail that encourages even more speculation with respect to atmospheric structure and dynamics.

In order to unambiguously interpret the Venus images, however, it is essential that we understand the basic nature of the UV contrasts. In particular, is the differential absorption of solar energy associated with the contrasts occurring above, below or within the visible clouds? Such a question is meaningful not only because of the impact its answer has on atmospheric dynamics, but also in view of the fact that at least some of the characteristics of the main visible cloud layer are reasonably well established. Thus, the determination that visual optical depth unity occurs at

approximately 50 mb (Hansen and Hovenier, 1974) provides us with a convenient reference point.

In this paper we consider in detail a number of possible models for the origin of the UV contrasts for the purpose of establishing whether observations presently available permit a definitive choice. Short of being able to select a specific model, we wish to determine the impact of not only present, but possible future observations on the acceptability of the various models. Before looking at specific models, we first examine several observations which have fundamental implications for any model considered.

2. Observations

a. Contrast and spherical albedo as a function of wavelength

The UV contrasts themselves are perhaps best characterized by the observed wavelength dependence of the degree of contrast. Fig. 1 summarizes the photometric data by Coffeen (1971) at 83° phase angle, the spectrophotometry by Woodman and Barker (1973) at 81° phase angle, and the two points based on ultraviolet and blue photographs by Ross (1928). Percentage contrast is defined following Coffeen as

$$C = 100(I_B - I_D)/I_B, \quad (1)$$

where I_B and I_D are the intensities of the bright and dark regions, respectively. The significant feature mani-

¹ Presented at the Conference on the Atmosphere of Venus, Goddard Institute for Space Studies, 15-17 October 1974.

fest in these data is the sharp decrease in contrast for wavelengths longward of about $\lambda=0.36 \mu\text{m}$, with a disappearance of dark regions by $\lambda=0.5-0.55 \mu\text{m}$. Although there may be evidence for somewhat higher contrasts in the visual region on rare occasions from ground-based observations (Kuiper *et al.*, 1969; Dollfus, 1975) and for specific polar features from Mariner 10 images (Hapke, 1974), the results shown in Fig. 1 probably represent typical conditions. Further, we note that the photographs of faint markings in the yellow shown by Kuiper *et al.* do not seem to indicate any correlation with UV markings observed at the same time. Since ground-based observations over a number of years indicate maximum contrasts of about 25% (Smith, 1975), and Coffeen (1971) reports that his observations were made when Venus showed a strong central dark region, we have adopted the dashed-line curve representing Coffeen's results as an appropriate relation for comparison to theoretical models.

It is often implicitly assumed that the mechanism causing the UV contrasts is at the same time responsible for the lower spherical albedo observed for wavelengths shortward of $\lambda=0.6 \mu\text{m}$. Thus, a careful examination of the wavelength dependence of the spherical albedo, especially in the ultraviolet, is warranted. Photoelectric measurements of the magnitude of Venus as a function of phase angle have been carried out by Irvine *et al.* (1968a, b) for ten wavelengths in the 0.3147 to 1.0635 μm region. Since the range of phase angles at which observations were made is restricted to 31.5° to 108.1° for wavelengths $\geq 0.6264 \mu\text{m}$, and 36.5° to 158.7° for the shorter wavelengths, Irvine's (1968) determination of the spherical albedo involves a least-squares cubic fit to the data to obtain the complete phase variation.

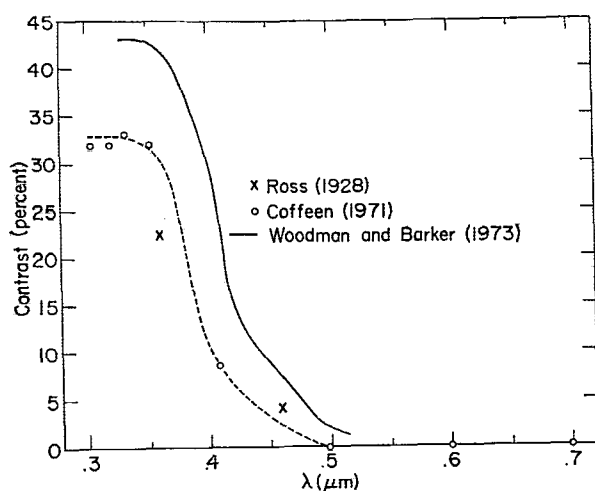


FIG. 1. Observations of the percentage contrast for Venus as a function of wavelength. Percentage contrast is defined as $100(I_B - I_D)/I_B$, where I_B and I_D are the intensities of the bright and dark areas, respectively. The dashed line representing the indicated points of Coffeen (1971) is adopted as an appropriate relation for comparison to theoretical models.

TABLE 1. Single scattering albedos and spherical albedos determined from the best fit of homogeneous, semi-infinite models to the observations of monochromatic magnitudes as a function of phase angle by Irvine *et al.* (1968a, b).

λ (μm)	$\tilde{\omega}$	A
0.3147	0.968865	0.49
0.3590	0.981563	0.56
0.3926	0.986806	0.61
0.4155	0.993681	0.71
0.4573	0.997382	0.80
0.5012	0.997995	0.82
0.6264	0.999963	0.97
0.7297	0.999841	0.95
0.8595	0.999568	0.92
1.0635	0.999166	0.88

In view of the fact that Hansen and Hovenier (1974) have since determined with reasonable certainty the properties of the cloud particles based upon polarization observations, we have instead calculated the spherical albedo using a homogeneous, semi-infinite model atmosphere² with the phase matrix appropriate for these particles. These multiple scattering models were computed using the doubling method (Hansen, 1971). The procedure thus involves only the variation of one number, the single scattering albedo $\tilde{\omega}$ of the cloud particles, until the best least-squares fit between the calculated magnitudes and observed values (Irvine *et al.*, 1968a, b) is obtained. Fig. 2 shows the comparison of the resulting best fit and the observations for each of the ten wavelengths. In Table 1 we give the single scattering albedos thus obtained and the spherical albedos A which immediately follow.

The OAO scanner observations of Venus at 103° phase angle reported by Wallace *et al.* (1972) allow us to extend the spherical albedo determination further into the ultraviolet. Since these measurements are relative rather than absolute, it is necessary to normalize them to the above results for $\lambda=0.3147 \mu\text{m}$. This introduces some uncertainty because the longest wavelength reached in the OAO observations is $\lambda=0.3 \mu\text{m}$, and we are therefore required to assume that the planetary magnitude for 103° phase angle is a smooth function of wavelength in this region. Since these observations are for a single phase angle, the determination of the spherical albedo now, of course, entails finding the single scattering albedo for which the model yields a fit to the one magnitude point. We have assumed throughout that n_r , the real part of the index of refraction for the cloud particles, can be specified for wavelengths shortward of $\lambda=0.365 \mu\text{m}$ by extrapola-

² The adequacy of the homogeneous model for our purposes is demonstrated by the close fit of our computations with the observations and by comparisons which Kawabata and Hansen (1975) have made between homogeneous and inhomogeneous models. For the present computations we have assumed that the ratio of the Rayleigh scattering coefficient within the cloud to the cloud particle scattering coefficient is $f_R=0.045$ at $\lambda=0.365 \mu\text{m}$.

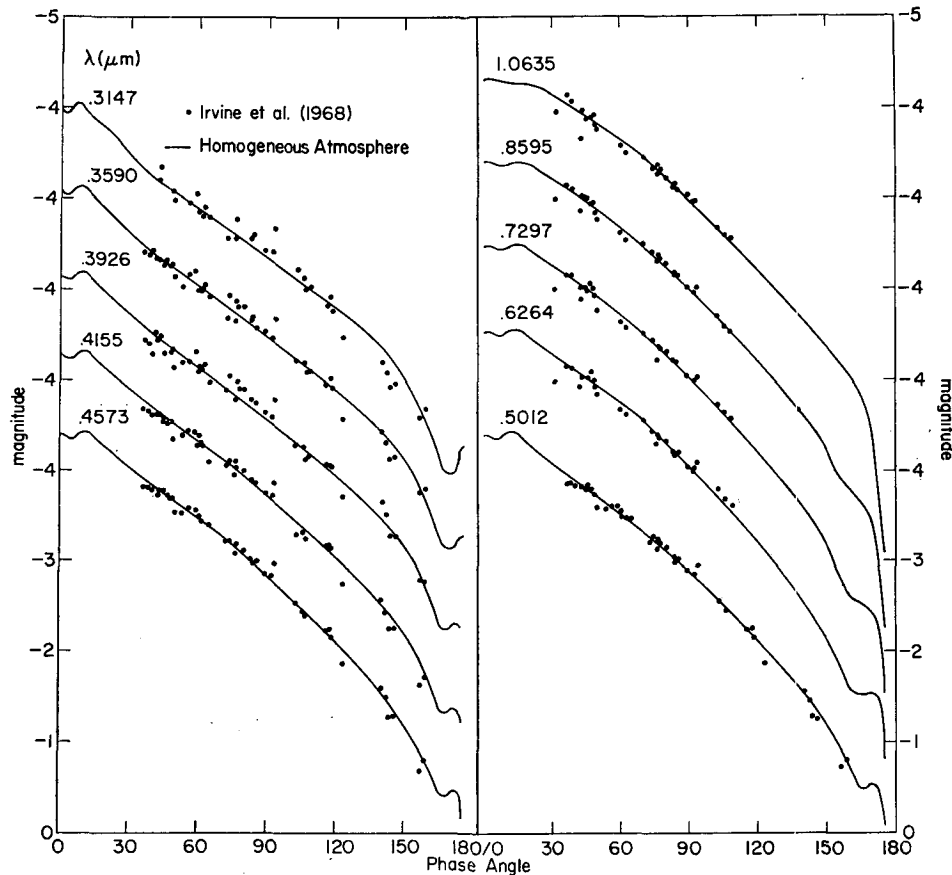


FIG. 2. Observations and theoretical relations of monochromatic magnitudes for Venus as a function of phase angle. The photometric observations by Irvine *et al.* (1968) at the ten indicated wavelengths are represented by dots. The theoretical curves are for a homogeneous model atmosphere with the single scattering albedo selected to yield the best fit to the observations.

tion of the dispersion relation given by Hansen and Hovenier (1974).

The spherical albedos thus determined are shown in Fig. 3, with the ten wavelength points based on the data of Irvine *et al.* (1968a, b) represented by filled circles and those based on the data of Wallace *et al.* (1972) by open circles. The latter are nine points from a smooth curve drawn through the 18 geometric albedo points actually shown by Wallace *et al.* For comparison, the broken line corresponds to a portion of the well-known compilation presented by Kuiper (1969); this has often been used in interpreting Venus cloud properties. His curve for this wavelength region represents Irvine's (1968) values for $\lambda \geq 0.359 \mu\text{m}$ and the results from Evans (1967) for the ultraviolet.

Except for the point at $\lambda = 1.0635 \mu\text{m}$, it may be noted that the present determination leads to values lying somewhat above the spherical albedos found by Irvine. This is primarily a consequence of our use of Johnson's (1965) value for the solar visual magnitude, $m_{\odot} = -26.74$, whereas Irvine adopted the $m_{\odot} = -26.81$ value given by Harris (1961). Eliminating this 6% difference, our values range from 0.01 higher at $\lambda = 0.3147$

μm to 0.03 and 0.06 lower at $\lambda = 0.6264$ and $1.0635 \mu\text{m}$, respectively, as a result of the difference between our procedure and the cubic fit employed by Irvine. The relative accuracy of the spherical albedos in the visual region should be about ± 0.03 , while uncertainties in calibration and the normalization for the UV values require an estimate of perhaps ± 0.06 for that region. Of course, the systematic effect due to the uncertain solar visual magnitude remains as well. Furthermore, one cannot completely discount the possibility that the discrepancies between the earlier rocket UV spectra (Evans, 1967; Jenkins *et al.*, 1969; Anderson *et al.*, 1969) and the OAO observations might be due to real temporal changes rather than simply improvements in measurements and calibration.

Two features of the spherical albedo as a function of wavelength which have a significant impact on the question of UV contrasts are the very high value (0.97) at $\lambda = 0.6264 \mu\text{m}$, and the broad absorption feature at shorter wavelengths with a minimum albedo near $\lambda = 0.3 \mu\text{m}$. Such a high albedo in the red implies nearly conservative scattering in a relatively thick cloud layer (cf. Lacy, 1975), and means that whatever causes the

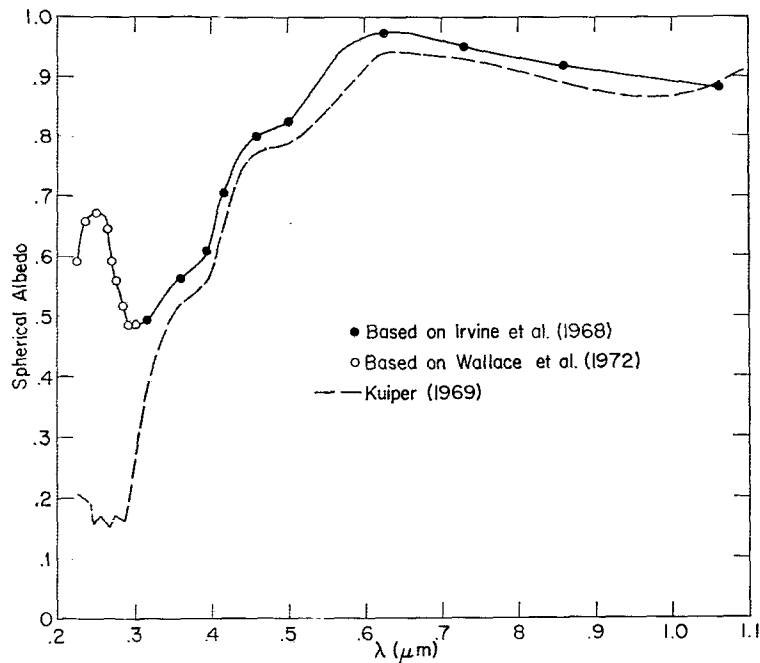


FIG. 3. Spherical albedo for Venus as a function of wavelength. Filled circles indicate spherical albedos determined from fitting theoretical model atmospheres to observations by Irvine *et al.* (1968) as shown in Fig. 2. Open circles represent points determined by fitting to the planetary magnitudes obtained by Wallace *et al.* (1972). The spherical albedo relation compiled by Kuiper (1969) is shown by the broken line.

absorption in the blue and ultraviolet must be almost completely transparent in this region. It is also useful to note that if the visible cloud particles provide the absorption, then for a homogeneous semi-infinite atmosphere, the imaginary part n_i of the index of refraction will range from a maximum of 7.56×10^{-4} at $\lambda = 0.293 \mu\text{m}$ to a minimum of 1.6×10^{-6} at $\lambda = 0.6264 \mu\text{m}$.

In Fig. 4 we reproduce the spherical albedo curve along with two other relations which are indicated by dashed lines and which form an envelope in the region of observed contrasts. These relations are based upon an assumption that will be made throughout; namely, that a reasonable average for contrasts over the disk and for varying phase angles is provided by comparing spherical albedos A_D and A_B obtained for the two extremes in which the disk is completely covered by the darkest, and then the brightest regions, respectively. Thus, the percentage contrast will be given by

$$C = 100(A_B - A_D)/A_B, \quad (2)$$

analogous to Eq. (1). The relation between A , the actual spherical albedo, and these extremes is then specified by our assumption that dark regions are uniformly distributed over the surface and that they constitute 25% of the surface area.³ Wavelength-dependent

³ Although images suggest that a somewhat greater percentage of the surface may be dark, the figure of 25% is intended to allow for the fact that not all dark regions correspond to the maximum contrast levels.

values of A_B and A_D are then computed for contrast levels specified by the dashed line representing Coffeen's (1971) observations in Fig. 1, and these define the envelope shown in Fig. 4. It is important to keep in mind the average nature of the contrast specified by A_B and A_D , and the consequence that larger and smaller contrasts on a local basis are consistent with our model.

A significant point illustrated in Fig. 4 is the fact that the magnitude of the contrast decreases much more rapidly with increasing wavelength than does the absorption required to produce the observed spherical albedo. For example, the percentage contrast decreases by more than a factor of 30 between $\lambda = 0.36$ and $0.5 \mu\text{m}$, whereas the corresponding decrease in the absorption is about a factor of 7. Also, the observations by Coffeen (1971) show that the contrast is essentially constant between $\lambda = 0.3557$ and $0.305 \mu\text{m}$, while we note that the albedo is decreasing from 0.56 to 0.49. Since this change in spherical albedo corresponds to a 54% increase in the absorption, one might expect to find the contrast increasing from 32% at $\lambda = 0.3557 \mu\text{m}$ to 49% at $\lambda = 0.305 \mu\text{m}$. These features indicate that it is quite likely that the mechanism causing the contrasts is not the sole agent responsible for the wavelength dependence of the spherical albedo. Rather, it appears that at least one other absorber, not localized to the regions of contrast, must be the primary source of absorption in the $\lambda = 0.45$ to $0.6 \mu\text{m}$ region, as well as

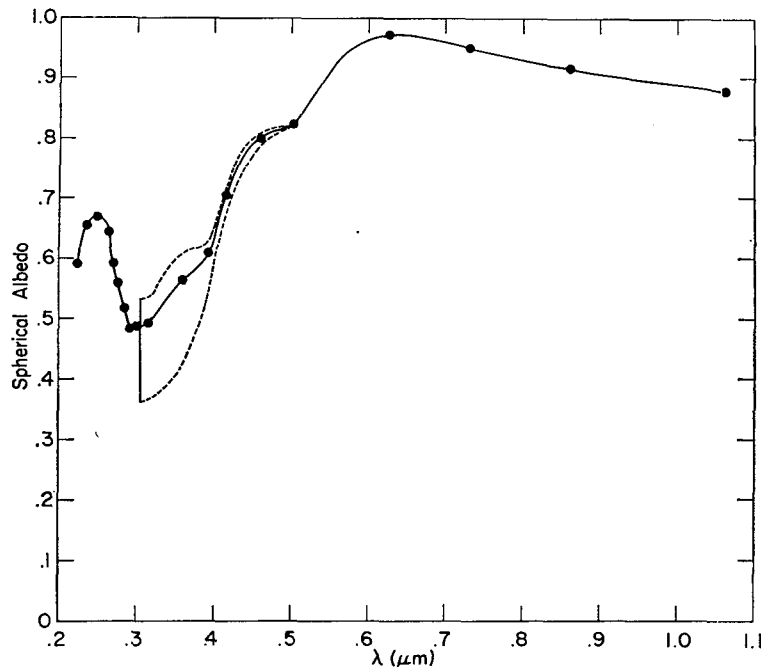


FIG. 4. Spherical albedo for Venus as a function of wavelength, and an envelope representing the maximum magnitude of the contrast. The solid line relation for the spherical albedo is reproduced from Fig. 3. The two dashed-line relations indicate the spherical albedos which would be obtained for the hypothetical situations in which the planet is completely covered by bright, and then dark, regions, respectively. It is assumed that the actual spherical albedo corresponds to the disk being about 25% covered by dark markings.

perhaps contributing in the ultraviolet. It is most difficult to conceive of a model for the contrasts in which a single absorber is capable of reducing the spherical albedo to 0.82 at $\lambda = 0.5 \mu\text{m}$ but producing the small or non-existent contrast observed there. Even if we adopt the higher contrast levels reported by Woodman and Barker (1973), this conclusion remains essentially the same.

b. Correlation of polarization with contrasts

One of the more significant clues regarding the nature of the contrasts may be the possible correlation of polarization with the bright and dark regions. Using a photographic subtraction method, Fountain (1974) has found that the brighter areas have a higher polarization than the darker regions for an observation made at 74° phase angle. On the other hand, for the same date Coffeen (cf. Coffeen and Hansen, 1974) finds the opposite effect using a scanning photometer/polarimeter. Since the rather difficult photographic subtraction method probably has a greater potential for error, it may be appropriate to consider Coffeen's result the more reliable in this uncertain situation.

Observations of the entire disk usually yield curves of polarization as a function of phase angle which exhibit little temporal variation except in the ultra-

violet (cf. Dollfus and Coffeen, 1970). Variation of the polarization at $\lambda = 0.365 \mu\text{m}$ since 1959 has been examined by Coffeen and Baker (1973) for the 41° – 127° phase angle range. They find that after adjustment for the explicit dependence on phase angle, the fluctuations may correspond to changes in the pressure at cloud optical depth unity of more than a factor of 2 on both a short and long term basis. Also, Bowell (1974) has observed small-amplitude variations in the polarization in the 60° – 80° phase angle region which may be correlated with the approximately 4-day variation in CO_2 absorption line strengths. These fluctuations can be interpreted as an approximately 3 mb variation in the pressure at the level of optical depth unity for the clouds.

Systematically smaller UV polarization observed during 1965 for the rainbow, or cloudbow, region around 15° phase angle (cf. Fig. 3 of Dollfus and Coffeen, 1970) cannot be attributed to differential Rayleigh scattering due to cloud height variation, however, in view of the small phase angles involved. Associating such a change with the UV contrasts must, of course, be speculative since the observations are of the entire disk. Such speculation is encouraged, however, by the preliminary Mariner 10 observation of polarization being a factor of 2 smaller for the dark areas for a phase angle near the rainbow (Hapke, 1974). If this is a firm result, it has

a very significant impact on the acceptability of some models for the origin of the contrasts. No model, however, should explain a possible correlation between contrasts and polarization at the expense of the excellent agreement that is obtained for disk-integrated observations with the homogeneous models used by Hansen and Hovenier (1974).

3. Physical models

a. Clouds of absorbing particles

Perhaps the most straightforward explanation for the contrasts might come from models in which the dark markings in the UV are simply clouds of absorbing aerosol particles distinct from the particles of the white visible cloud layer. Such a model would seem natural if one shares the widely held belief that the main cloud layer particles can be identified as a concentrated solution of sulfuric acid (cf. Sill, 1972; Young, 1973, 1974; Prinn, 1973; Hansen and Hovenier, 1974; Martonchick, 1974) and therefore do not have significant absorption in the ultraviolet or visual wavelength regions (cf. Palmer and Williams, 1975). This of course assumes that there is no impurity dissolved in the sulfuric acid which could cause the requisite absorption.

Consider first a model in which the absorbing clouds lie below the white visible clouds. In this case it is assumed that a uniform layer of absorbing clouds lies below the conservative scattering upper layer, whose optical thickness varies in order that the appropriate contrast can be obtained. Fig. 4 indicates that at $\lambda=0.365 \mu\text{m}$, the albedo of the lower, absorbing portion of the atmosphere should be $A_D=0.43$, corresponding to the darkest regions. When a layer of the white visible clouds with $\bar{\omega}=1.0$ and of optical thickness $\tau=4$ is added on top of this lower layer, a spherical albedo of $A_B=0.64$ is obtained. Thus, this model can produce the desired maximum contrast of 30% at $\lambda=0.365 \mu\text{m}$ with a variation in optical thickness of the main visible cloud layer between zero and slightly less than $\tau=4$. The change in the magnitude of the contrast as a function of wavelength may be achieved by the appropriate wavelength dependence of the absorption in the lower clouds.

In principle, a similar result can be obtained if the albedo of the lower, absorbing region is decreased and compensated by an increase in the thickness of the upper, white clouds. However, such a possibility should be considered in light of the Mariner 10 observation (Hapke, 1974) that dark regions may have lower polarization for phase angles near the rainbow. The basic features of the curve of polarization as a function of phase angle are dependent on only the topmost region of any scattering medium. Differences below optical depth on the order of unity have an effect only in that absorption in the lower levels decreases the intensity, resulting in an increase in the magnitude of the per-

centage polarization. Obviously, this means that the opposite of the observed result is obtained unless there is a small optical thickness of the conservative scattering cloud above the absorbing cloud layer for the dark regions.

If the polarization is actually less for the dark regions, then the model with a lower absorbing layer requires clear regions in the white visible clouds. Because of the diffuse nature of the visible clouds (cf. Kawabata and Hansen, 1975) this implies that the clear region would have to extend down to about the 150 mb level, with an optical depth due to Rayleigh scattering of $\tau_R \approx 0.15$ above the absorbing cloud layer. One would therefore expect to find the CO_2 absorption being significantly stronger over the dark features. Although some observations (Young *et al.*, 1973; Barker, 1974) have indicated an approximately 4-day periodicity in CO_2 line strengths at some times, there is doubt (Young, 1975a, b) that this corresponds to a rapid rotation of the upper cloud region inferred from the apparent motion of the UV markings. The only evidence supporting a correlation between contrasts and CO_2 variations seems to be a single observation by Young *et al.* (1974) indicating more CO_2 at 54° north latitude, while bright regions were noted at high latitudes on the UV photographs. It therefore appears that a model with such clear spaces in the upper visible clouds is inconsistent with the CO_2 absorption line observations. Furthermore, although the polarization in the rainbow would be noticeably decreased, unacceptably high values on the order of +25% would be predicted for the 90° phase angle region due to the increased Rayleigh scattering.

The situation is somewhat improved for the model in which the absorbing clouds are within the principal cloud layer. In this case we assume that the absorption is occurring not in a well-defined layer, but in discrete clouds whose position relative to the top of the white, main cloud layer is variable. Thus, one of the dense absorbing clouds within a fraction of a kilometer of the top would correspond to the darkest region, and one at the 150 mb level below, to a bright area. Although the question of dispersal and mixing of the absorbing clouds would require some consideration, it is perhaps not too unreasonable to draw an analogy from water clouds within diffuse terrestrial hazes. With this model it is possible to obtain a lower polarization in the rainbow for the dark markings without the difficulties associated with a significant amount of gas overlying the absorbing cloud. The polarization for the darkest regions is essentially determined by the scattering properties of the particles making up the absorbing cloud.

As a specific example, we have constructed a model which has absorbing clouds composed of spherical particles with $n_r=1.46$ and $n_i=0.015$ at $\lambda=0.365 \mu\text{m}$ and a standard gamma size distribution with effective radius $r_{\text{eff}}=1.05 \mu\text{m}$, and variance $v_{\text{eff}}=0.07$ (cf. Hansen and Travis, 1974). These particles therefore have single

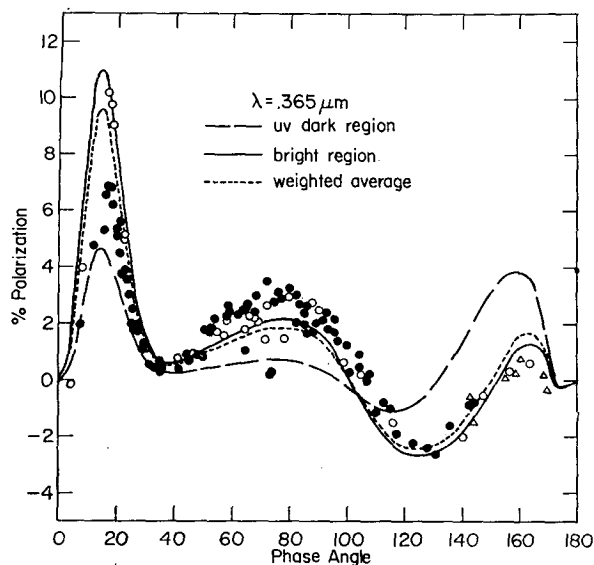


FIG. 5. Observations and theoretical computations of the polarization of sunlight reflected by Venus at $\lambda=0.365 \mu\text{m}$. Intermediate bandwidth filter observations by Coffeen and Gehrels (1969) are shown by filled circles, and those by Coffeen (cf. Dollfus and Coffeen, 1970) by open circles. The observations (Δ 's) of Dollfus (cf. Dollfus and Coffeen, 1970) and the four points of Coffeen for phase angles greater than 139° are for a region near the center of the intensity equator rather than the complete disk. The theoretical curves are for a model with clouds of absorbing particles floating within the main visible cloud layer. Such a cloud at the very top produces the darkest region, whose polarization is represented by the broken line. The weighted average of bright and dark regions is shown by the dashed line and should be compared with the observations of the entire disk.

scattering albedo $\bar{\omega}=0.6903$, so that a layer of optical thickness $\tau_a=0.8$ at the top of the thick, conservatively scattering, white clouds yields a spherical albedo of $A_D=0.43$. A value of $n_i=0.015$ not only provides the low value of $\bar{\omega}$ for the contrast-producing absorption, but also results in an appropriate reduction in the single scattering polarization in the rainbow for these particles. Our arbitrary selection of particles identical to those of the main cloud layer except for the non-zero n_i has the advantage that as n_i is decreased for increasing wavelength to correspond to smaller contrast levels, the scattering properties of these particles become more like those of the visible cloud particles. Consequently, we avoid any difficulty with respect to possibly undesirable effects on the polarization at the visual wavelengths.

Fig. 5 illustrates the results for polarization vs phase angle obtained for a model with the absorbing clouds composed of the particles specified above. The broken-line curve for an absorbing cloud at the very top of the main cloud layer does indeed indicate a significantly lower polarization in the rainbow region around 15° phase angle than that for the solid line representing the bright areas. For comparison, observations of the entire disk by Coffeen and Gehrels (1969) and Dollfus

and Coffeen (1970) are shown as well as the dashed line representing a weighted average of the bright and dark areas, assuming that dark regions cover 25% of the disk. Note that the effect of the dark regions on the weighted average for the polarization is somewhat less than 25% because of their lower intensities.

Although the present model does lead to lower polarization for the darkest regions, the opposite becomes true for some of the dark areas corresponding to less than maximum contrast levels. This is actually a result of two competing effects: the lower polarization characteristic of the absorbing clouds, and the previously mentioned tendency for polarization to increase for clouds with absorption below them. Thus, for some contrast levels less than 30%, the absorbing cloud lies at a great enough depth so that the effect of its characteristic polarization is diminished, while the portion of the main cloud layer above it contributes an even higher polarization because of the absorption underneath. Specifically, in this model the polarization at 15° phase angle for a dark region increases from 4.6% at 30% contrast to 11% for 21% contrast. For still smaller contrasts, the polarization is found to be slightly higher than that for bright regions, reaching a maximum value for contrast of about 15% before dropping back to 11% at zero contrast.

It should be noted that if the present model is restricted to the inclusion of a single absorber, it is then necessary for all regions to have an absorbing cloud at some point below. This is required because the assumed $\bar{\omega}=1.0$ value for the main cloud layer necessitates absorption below or within in order to obtain a spherical albedo of 0.61 at $\lambda=0.365 \mu\text{m}$ for the bright regions. In view of the very scattered vertical distribution of absorbing clouds implicit in the model, it is perhaps questionable that the uniform horizontal distribution needed to fulfill this condition is likely to occur. At the same time, we find that when $\bar{\omega}$ for the absorbing clouds is chosen to give the observed spherical albedo at $\lambda=0.5 \mu\text{m}$, such a restriction on this model results in the prediction of a 5% contrast level for that wavelength. As this corresponds to an absorbing cloud which produces 30% contrast at $\lambda=0.365 \mu\text{m}$, the result would be even higher than 5% if we were to assume larger contrast levels in the UV. Since the observations (cf. Fig. 1) for $\lambda=0.5 \mu\text{m}$ show contrast levels well below 5%, the addition of a second absorber, unrelated to the contrast-producing one, is required to make this model more consistent with the observed contrasts.

The third possibility for the present category of models is for the absorbing clouds to lie above the principal visible clouds. In this case the range of contrasts is to be attributed to a horizontal variation in the optical thickness of this upper layer. If only one absorber is permitted in this model, absorbing clouds composed of the particles specified above must have an optical thickness $\tau_a=0.8$ over the dark areas and approximately $\tau_a=0.45$ over the brightest regions in

order to produce both the observed contrasts and spherical albedo at $\lambda=0.365 \mu\text{m}$. With a minimum optical thickness of 0.45, the polarization of not just the dark areas, but of the entire disk would be altered to a degree incompatible with observations. To some extent, such a difficulty can be alleviated by choosing particles with a smaller value of $\bar{\omega}$ than that obtained for $n_i=0.015$. By decreasing the requisite optical depth, this reduces the effect on the polarization due to scattering from the absorbing cloud layer.

An alternate approach is to allow a second source of absorption within or below the main cloud layer. This source of absorption is assumed to be distributed uniformly in the horizontal sense and could, for example, be of sufficient magnitude to give the spherical albedo of 0.61 at $\lambda=0.365 \mu\text{m}$ for bright regions without requiring further absorption from clouds above the main visible layer. Thus, the contrasts would be produced by the absorbing clouds lying above the main cloud layer and having optical thicknesses ranging from zero to $\tau_a \approx 0.3$. This allows the polarization for the bright regions to be unaffected. Note that this model requires, again, the presence of a second absorber.

b. Particle size variation

For this type of model, the contrast-producing absorption is to be found within the visible cloud layer particles themselves. Naturally, this implies the presence of a dissolved impurity if the particles are actually concentrated sulfuric acid solutions. Because of the restrictions on the particle characteristics from the analysis of polarization (cf. Hansen and Hovenier, 1974), such an impurity must have very little effect on the optical properties other than n_i .

For particles which have a small amount of absorption characterized by n_i on the order of 10^{-4} to 10^{-3} , the contrasts may be caused by regions of the cloud simply having slightly different effective particle sizes. This is brought about by the larger absorption, and hence smaller $\bar{\omega}$ for the larger particles, with a region containing an excess of such particles therefore appearing darker.

In order that agreement be maintained within the constraints on the cloud particle characteristics determined from the disk-integrated observations, it is assumed that the darkest and brightest regions correspond to higher concentrations of larger and smaller particles, respectively, from the "average" particle distribution. In our present model we therefore take the effective radii for the two extreme distributions to be given by $r_{\text{eff}} = 1.05 \mu\text{m} \pm \Delta r_{\text{eff}}$, and an effective variance of $v_{\text{eff}} = 0.03$. These two distributions are naturally assumed to be narrower than the average distribution with $v_{\text{eff}} = 0.07$. The assumed value of $n_i = 4.86 \times 10^{-4}$ at $\lambda = 0.355 \mu\text{m}$ is based upon the observed spherical albedo and the semi-infinite model (cf. Section 2). Fig. 6 illustrates the variation in r_{eff} required to achieve a

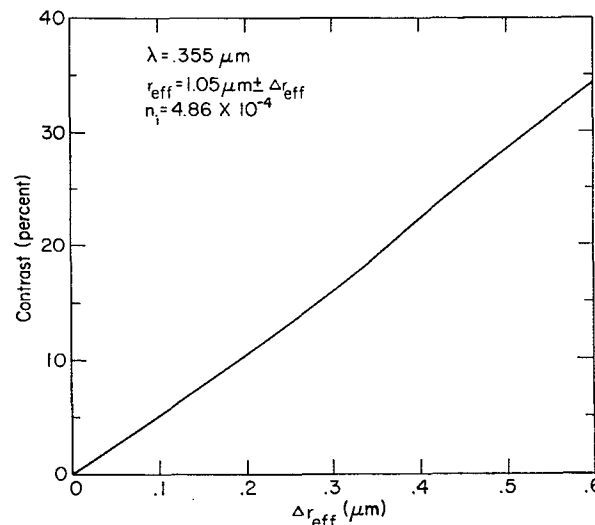


FIG. 6. Percentage contrast as a function of the magnitude of the size variation in the main cloud layer particles. The maximum contrast obtained at $\lambda=0.355 \mu\text{m}$ for a semi-infinite cloud model with $n_i=4.86 \times 10^{-4}$ is shown for effective radius variations up to $0.6 \mu\text{m}$.

given contrast level for a model in which the cloud layer is assumed to be semi-infinite. The nearly linear relation indicates that $\Delta r_{\text{eff}} = 0.54 \mu\text{m}$ is sufficient to produce the maximum contrast of 31% appropriate for $\lambda = 0.355 \mu\text{m}$.

The standard particle distribution with $r_{\text{eff}} = 1.05 \mu\text{m}$ and $v_{\text{eff}} = 0.07$ has a standard deviation of $\sigma = 0.26 \mu\text{m}$. Since very few particles in the distribution have radii deviating by more than 2σ from the effective radius, a value of $\Delta r_{\text{eff}} = 0.54 \mu\text{m}$ may be considered somewhat large for sufficient regions of contrast to be formed. This is not a fundamental problem, however, because the contrast for a given Δr_{eff} increases approximately proportional to $n_i^{3/2}$, and the value for n_i is somewhat arbitrary. Taking into consideration the smaller surface area covered by the darkest regions and the possibility that the cloud layer is finite in thickness, it may be reasonable to assume a value for n_i which is a factor of 2 to 3 higher than the 4.86×10^{-4} used here. Furthermore, we note that if the value of n_i for $\lambda = 0.5 \mu\text{m}$ determined from the spherical albedo and the semi-infinite approximation is used, a contrast of about 15% is predicted by this model in comparison to the nearly zero contrast level observed for that wavelength. This indicates that a second source of absorption is required, perhaps lying below the finite cloud layer in which the particle size variation produces the contrasts.

Regarding the question of polarization, this model predicts a higher polarization in the rainbow for dark regions rather than the lower value reported by Hapke (1974). This is a result of the fact that for particle sizes on the order of $1 \mu\text{m}$, the single scattering phase matrix gives a greater polarization for the larger par-

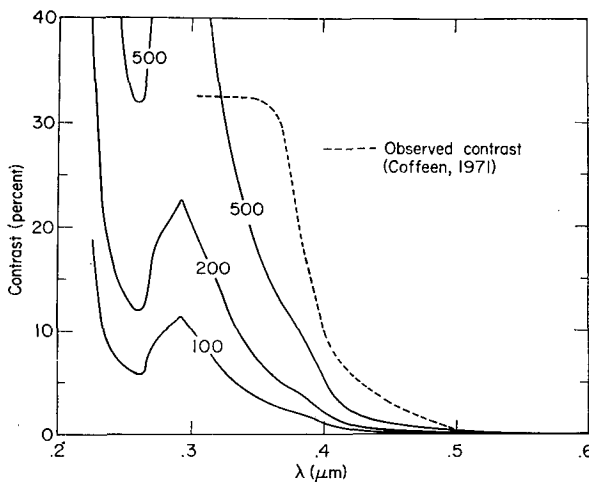


FIG. 7. Percentage contrast as a function of wavelength for models in which the cloud tops vary significantly in altitude. The three model relations indicated are for 100, 200 and 500 mb of gas above the lowest clouds. The observed contrast is represented by the dashed line (cf. Fig. 1).

ticles, which in this model correspond to the dark regions. Accordingly, whether this model can be acceptable or not must depend upon the actual differential in polarization between bright and dark markings. There should be little difficulty in obtaining the appropriate disk-integrated polarization with this model because of our requirement that the extreme particle distributions be composed of particles taken from the average distribution specified by the observations of the entire disk. Thus, the average over bright and dark regions will be nearly the same as that obtained from a region in which the particles of these distributions are mixed.

c. Particle number density variation

Here we again assume that the contrast-producing absorption is in the particles of the main visible cloud layer. The contrast is assumed to be a result of horizontal variation in the number density of particles in a finite cloud layer. The resulting variation in the optical depth above a lower, uniform region differs from that given in Section 3a only in that the absorption is now due to the visible cloud layer particles themselves. An appropriate choice for the value of n_i depends upon two factors. For a given n_i , the spherical albedo required for the bright regions limits the maximum optical thickness allowed for this upper cloud layer. However, these clouds must be at least thick enough so that they are the dominant factor in determining the polarization. At the same time, n_i cannot be so large that the single scattering polarization is significantly affected. It is therefore appropriate to limit n_i to values on the order of 10^{-3} . If for example, we take $n_i = 10^{-3}$ for $\lambda = 0.365 \mu\text{m}$ and assume a relatively small

absorption below, a main cloud layer with τ varying between about 3 and 6 is sufficient to produce the observed contrast. This amounts to only a factor of 2 variation in the particle number density, a value which is perhaps not unreasonable even for fairly diffuse clouds.

The predicted polarization in the rainbow region for the dark areas in this type of model is higher than that for the bright features. This is, of course, the familiar result of the increase in the percentage polarization corresponding to the decrease in intensity due to absorption lower in the cloud. One interesting aspect of this model is the fact that the polarization in the 40° – 120° phase angle range will be lower for the dark regions. In a homogeneous model one assumes a constant mixing ratio of the cloud particles to the molecular atmospheric constituents, and this can be specified by f_R , the ratio of the Rayleigh scattering coefficient to the cloud particle scattering coefficient (cf. Hansen and Hovenier, 1974). For the diffuse visible clouds, this contribution due to Rayleigh scattering actually dominates the polarization in the 40° – 120° phase angle region. Since the value of f_R for dark areas in the present model must be lower because of the greater number density of the cloud particles, these regions should therefore exhibit lower polarization.

d. Cloud height variation

Because of the wavelength dependence of the observed contrasts, it is often suggested that cloud height variation and the accompanying differential effect of Rayleigh scattering might be the cause. The absorption is assumed to be within or below the main cloud layer and due to either the cloud particles themselves or other absorbing particles. If the cloud tops vary in height relative to the gaseous atmosphere, then the lower clouds will appear brighter due to the excessive Rayleigh scattering above them. The dark features are clouds with very little gas above them and having sufficient absorption to give spherical albedos corresponding to the lower curve of the envelope in Fig. 4.

In Fig. 7 we illustrate the results for the contrast as a function of wavelength for three models of this type. As indicated on the solid line relations, these three are distinguished by the amount of gas above the lowest cloud: 100, 200 and 500 mb. The models are based on the assumption of a semi-infinite cloud layer in which the particles themselves are the source of absorption. For comparison, the observations by Coffeen (1971) are represented by the dashed line. It is apparent that for $\lambda \gtrsim 0.325 \mu\text{m}$, in excess of 500 mb is required in order to obtain the observed contrast levels. Having the tops of the clouds which correspond to bright regions at a level below 500 mb is simply incompatible with other observations. The polarization would be grossly affected, becoming characteristic of Rayleigh scattering alone. Also, this model would predict unrealistically high CO_2

absorption line strengths and the rotational temperatures inferred from them, as well as a very strong correlation with bright areas. Moreover, there is no single choice for the amount of gas above the lowest clouds which will give the correct wavelength dependence for the contrasts. Models of this type can therefore be ruled out as explanations for the UV contrasts.

4. Conclusions

It must be concluded that present observational evidence simply does not permit a definitive choice between models attempting to explain the UV contrasts. Although we are able to rule out models relying on differential Rayleigh scattering due to large cloud height variations, a number of viable alternatives remain. Therefore, no specific answer can be given for the question of the location of the contrast-producing absorber relative to the visible clouds. The possibility raised by a preliminary Mariner 10 observation (Hapke, 1974) that dark regions have a lower polarization for phase angles near the rainbow has important implications. If confirmed, this observation considerably narrows the field of potentially acceptable models. Only models with absorbing particles distinct from the particles of the main visible cloud layer seem capable of yielding this type of behavior.

On the basis of the wavelength dependence of both the degree of contrast and the spherical albedo, we conclude that any of the acceptable models probably requires at least one source of absorption other than the one responsible for the contrasts. Additional observations of the magnitude of the contrast in the $\lambda=0.35\text{--}0.6\ \mu\text{m}$ range during times when particularly dark features are noted would permit increased certainty in this question. This point has relevance not only to the question of the spectral dependence of the contrast-producing absorber, but also to the location of the solar heating of the atmosphere. If more than one source of absorption is required, it is then likely that of the approximately 22% of the incident solar flux absorbed by the atmosphere, the contrast-producing absorber accounts for only a very small fraction (cf. Lacis, 1975). In this regard, observations to improve the wavelength resolution in the $\lambda=0.35\text{--}0.6\ \mu\text{m}$ region for the spherical albedo curve would also be useful.

Without definite knowledge of the mechanism responsible for the contrasts and the location of the necessary absorption, any interpretation of the apparent cloud motion and its import for atmospheric structure and dynamics must remain speculative. In order for further progress to be made in the analysis of possible origins of the contrasts, a great deal more information must be acquired. Most of our present data refer to the entire disk, whereas the more difficult observations establishing differences between bright and dark features are needed. Observations of the differences in polarization between bright and dark regions

should prove to be one of the most useful in the search for a definitive model.

There are, of course, limitations on ground-based observations. For example, some of the most informative polarization measurements are those near the rainbow of the Venus clouds at about 15° phase angle, where it becomes quite difficult to isolate dark regions on the disk in ground-based observations. The first close-up view provided by Mariner 10 has resulted in a number of potentially significant observations although the TV system was not designed to do polarimetry. It is to be expected that extensive polarization measurements along with the imaging, UV, and IR observations from the future Pioneer Venus orbiter will furnish sufficient information so that the characteristics of the local areas associated with the contrasts can be determined. Also, the Pioneer Venus entry probes, as well as orbiter observations of local areas from different parts of the orbit, should provide details on the vertical structure. Observations such as these should provide for a great improvement over our present uncertainty regarding the origin of the UV contrasts.

Acknowledgments. The author is indebted to Drs. J. Hansen, A. Lacis and K. Kawabata for helpful suggestions and substantial contribution to this paper.

REFERENCES

- Anderson, R. C., J. G. Pipes, A. L. Broadfoot and L. Wallace, 1969: Spectra of Venus and Jupiter from 1800 to 3200 Å. *J. Atmos. Sci.*, **26**, 874-888.
- Barker, E. S., 1974: Semi-periodic variations in CO₂ abundance on Venus. *Bull. Amer. Astron. Soc.*, **6**, 367.
- Bowell, E., 1974: Short-term periodic variations in the polarization of Venus. Presented at the Conference on the Atmosphere of Venus.
- Boyer, C., and H. Camichel, 1961: Observations photographiques de la planète Venus. *Ann. Astrophys.*, **24**, 531-535.
- , and P. Guerin, 1969: Étude de la rotation rétrograde, en 4 jours, de la couche extérieure nuageuse de Venus. *Icarus*, **11**, 338-355.
- Coffeen, D. L., 1971: Venus cloud contrasts. *Planetary Atmospheres*, C. Sagan, T. C. Owen, H. J. Smith, Eds., Dordrecht, Netherlands, Reidel, 84-90.
- , and A. L. Baker, 1973: Venus: Ultraviolet polarization variations. *Bull. Amer. Astron. Soc.*, **5**, 301.
- , and T. Gehrels, 1969: Wavelength dependence of polarization. XV. Observations of Venus. *Astron. J.*, **74**, 433-445.
- , and J. E. Hansen, 1974: Polarization studies of planetary atmospheres. *Planets, Stars and Nebulae Studied with Photopolarimetry*, T. Gehrels, Ed., University of Arizona Press, 518-581.
- Dollfus, A., 1975: Venus: Evolution of the upper atmospheric clouds. *J. Atmos. Sci.*, **32**, 1060-1070.
- , and D. L. Coffeen, 1970: Polarization of Venus. I. Disk observations. *Astron. Astrophys.*, **8**, 251-266.
- Evans, D. C., 1967: Ultraviolet reflectivity of Venus and Jupiter. *Moon and Planets*, A. Dollfus, Ed., Amsterdam, North-Holland, 135-149.
- Fountain, J. W., 1974: Spatial distribution of polarization over the disks of Venus, Jupiter, Saturn, and the Moon. *Planets, Stars and Nebulae Studied with Photopolarimetry*, T. Gehrels, Ed., University of Arizona Press, 223-231.

- Hansen, J. E., 1971: Multiple scattering of polarized light in planetary atmospheres. Part I. The doubling method. *J. Atmos. Sci.*, **28**, 120-125.
- , and J. W. Hovenier, 1974: Interpretation of the polarization of Venus. *J. Atmos. Sci.*, **31**, 1137-1160.
- , and L. D. Travis, 1974: Light scattering in planetary atmospheres. *Space Sci. Rev.*, **16**, 527-610.
- Hapke, B., 1974: Mariner 10 photometry. Presented at the Conference on the Atmosphere of Venus.
- Harris, D. L., 1961: Photometry and colorimetry of planets and satellites. *Planets and Satellites*, G. P. Kuiper and B. M. Middlehurst, Eds., University of Chicago Press, 272-342.
- Irvine, W. M., 1968: Monochromatic phase curves and albedos for Venus. *J. Atmos. Sci.*, **25**, 610-616.
- , T. Simon, D. H. Menzel, J. Charon, G. Lecomte, P. Griboval and A. T. Young, 1968a: Multicolor photoelectric photometry of the brighter planets. II. Observations from Le Houga Observatory. *Astron. J.*, **73**, 251-264.
- , —, —, C. Pikoos and A. T. Young, 1968b: Multicolor photoelectric photometry of the brighter planets. III. Observations from Boyden Observatory. *Astron. J.*, **73**, 807-828.
- Jenkins, E. B., D. C. Morton and A. V. Sweigart, 1969: Rocket spectra of Venus and Jupiter from 2000 to 3000 Å. *Astrophys. J.*, **157**, 913-924.
- Johnson, H. L. 1965: The absolute calibration of the Arizona photometry. *Comm. Lunar Planet. Lab.*, No. 53, 73-77.
- Kawabata, K., and J. E. Hansen, 1975: Interpretation of the variation of polarization over the disk of Venus. *J. Atmos. Sci.*, **32**, 1133-1139.
- Kuiper, G. P., 1969: Identification of the Venus cloud layers. *Comm. Lunar Planet. Lab.*, No. 101, 229-250.
- , J. W. Fountain and S. M. Larson, 1969: Venus photographs. I. Photographs of Venus taken with the 82-inch telescope at McDonald Observatory, 1950-56. *Comm. Lunar Planet. Lab.*, No. 102, 251-262.
- Lacis, A. A., 1975: Cloud structure and heating rates in the atmosphere of Venus. *J. Atmos. Sci.*, **32**, 1107-1124.
- Martonchik, J. V., 1974: Sulfuric acid cloud interpretation of the infrared spectrum of Venus. *Astrophys. J.*, **193**, 495-501.
- Murray, B. C., M. J. S. Belton, G. E. Danielson, M. E. Davies, D. Gault, B. Hapke, B. O'Leary, R. G. Strom, V. Suomi and N. Trask, 1974: Venus: Atmospheric motion and structure from Mariner 10 pictures. *Science*, **183**, 1307-1315.
- Palmer, K. F., and D. Williams, 1975: Optical constants of sulfuric acid: Application to the clouds of Venus? *Appl. Opt.*, **14**, 208-219.
- Prinn, R. G., 1973: Venus: Composition and structure of the visible clouds. *Science*, **182**, 1132-1134.
- Ross, F. E., 1928: Photographs of Venus. *Astrophys. J.*, **67**, 57-92.
- Scott, A. H., and E. J. Reese, 1972: Venus: Atmospheric rotation. *Icarus*, **17**, 589-601.
- Sill, G. T., 1972: Sulfuric acid in the Venus clouds. *Comm. Lunar Planet. Lab.*, No. 171, 191-198.
- Smith, B. A., 1967: Rotation of Venus: Continuing contradictions. *Science*, **158**, 114-116.
- , 1975: Ground-based observations of ultraviolet clouds on Venus. To be submitted to *J. Atmos. Sci.*
- Wallace, L., J. J. Caldwell, and B. D. Savage, 1972: Ultraviolet photometry from the Orbiting Astronomical Observatory. III. Observations of Venus, Mars, Jupiter, and Saturn longward of 2000 Å. *Astrophys. J.*, **172**, 755-769.
- Woodman, J. H., and E. S. Barker, 1973: Relative spectrophotometry of ultraviolet clouds on Venus. *Bull. Amer. Astron. Soc.*, **5**, 301.
- Wright, W. H., 1927: Photographs of Venus made by infrared, and by violet light. *Publ. Astron. Soc. Pac.*, **39**, 220-221.
- Young, A. T., 1973: Are the clouds of Venus sulfuric acid? *Icarus*, **18**, 564-582.
- , 1974: Venus clouds: Structure and composition. *Science*, **183**, 407-409.
- , 1975a: Is the four-day "rotation" of Venus illusory? *Icarus*, **24**, 1-10.
- , 1975b: The clouds of Venus. *J. Atmos. Sci.*, **32**, 1125-1132.
- , A. Woszczyk and L. G. Young, 1974: Spectroscopic observations of spatial and temporal variations on Venus. *Acta Astron.*, **24**, 55-68.
- Young, L. G., A. T. Young, J. W. Young and J. T. Bergstralh, 1973: The planet Venus: A new periodic spectrum variable. *Astrophys. J.*, **181**, L5-L8.